FERMILAB-CONF-19-656-ND-PPD
ACCEPTED

Prepared for submission to JINST

15^{TH} Topical Seminar on Innovative Particle and Radiation Detectors
14-17 October 2019
Siena, Italy

Muon radiography applied to volcanoes imaging: the MURAVES experiment at Mt. Vesuvius

M. D'Errico,[a,b] F. Ambrosino,[a,b] G. Baccani,[c,d] L. Bonechi,[d] A. Bross,[e] M. Bongi,[c,d] A. Caputo,[f] R. Ciaranfi,[d] L. Cimmino,[a,b] V. Ciulli,[c,d] R. D'Alessandro,[c,d] F. Giudicepietro,[f] S. Gonzi,[c,d] G. Macedonio,[f] V. Masone,[b] B. Melon,[c,d] N. Mori,[c,d] P. Noli,[b] M.Orazi,[f] G. Passeggio,[b] R. Peluso,[f] A. Pla-Dalmau,[e] G. Saracino,[a,b] G. Scarpato,[f] L. Scognamiglio,[b] P. Strolin,[a,b] E. Vertechi,[f] and L. Viliani.[c,d]

[a] *University of Naples Federico II, Naples, Italy.*
[b] *INFN sez. di Napoli, Naples, Italy.*
[c] *University of Florence, Florence, Italy.*
[d] *INFN sez. di Firenze, Florence, Italy.*
[e] *Fermilab, Batavia, Illinois, USA.*
[f] *INGV, sez. di Napoli - Osservatorio Vesuviano, Naples, Italy.*

E-mail: mederrico@na.infn.it

Abstract: Muon radiography is a technique based on the measurement of absorption profiles of muons as they pass through matter. This measurement allows to obtain an image of the inner structure of large volume objects and is suitable to be applied in several fields, such as volcanology, archaeology and civil engeneering. One of the main applications concerns the study of volcanic structures; indeed it is possible to use this technique to measure the mass distribution inside the edifice of a volcano providing useful information to better understand the possible eruption mechanisms. The MURAVES (MUon RAdiography of VESuvius) project aims to the study of the summital cone of Mt. Vesuvius near Naples in Italy, one of the most dangerous active volcanoes in the world. The MURAVES apparatus is a modular, robust muon hodoscope system with a low power consumption, optimized to be used in inhospitable environments like the surroundings of volcanoes. The complete detection system is an array of identical tracking modules, each with an area of 1 m^2, based on the use of plasic scintillators. The technologies, the status and the data analysis strategy of the experiment will be presented in this paper.

This manuscript has been authored by Fermi Research Alliance, LLC under Contract No. DE-AC02-07CH11359 with the U.S. Department of Energy, Office of Science, Office of High Energy Physics.

Contents

1 Introduction

Muon radiography, or "muography", is based on the measurement of the absorption of muons in traversing the object under investigation. It is conceptually similar to the usual X-ray radiography, but with extended capabilities of investigating over much larger thicknesses of matter thanks to the penetrating power of high-energy muons. Instead of X-rays, muography exploits muons produced in the interactions of high-energy cosmic rays with the Earth's atmosphere. The first application of this technique was realized in 1970 by the Nobel prize Alvarez and collaborators [1] to search for unknown burial chambers in the Chephren's pyramid. The result of the study was that no chambers exist in the mass of limestone investigated by muon absorption. This study represents a milestone in the development of muography.

In recent years the possibility to apply this technique, using quasi-horizontal muons, to investigate the internal structure of volcanoes has been demonstrated by Tanaka [2–5] and other groups [6–8]. The spatial resolution that, in optimal conditions, can be obtained with this method is of the order of 10 m, which is difficult to achieve with the standard techniques used in geology.

In 2012, our collaboration, which involves physicists, geologists and volcanologists from Istituto Nazionale di Geofisica e Vulcanologia (INGV), Istituto Nazionale di Fisica Nucleare (INFN), the University of Florence and the University of Naples, submitted to the Italian Ministry of Research a proposal for a muographic and gravimetric measurements campaign on Vesuvius with the purpose of better defining the volcanic plug at the bottom of the crater. The proposal was approved and the project was named the MUon RAdiography of VESuvius (MURAVES) [9–11]. Funds were allocated in 2015 (Progetto Premiale decreto MIUR n. 949/ric del 19.12.2012, CUP D54G14000110001).

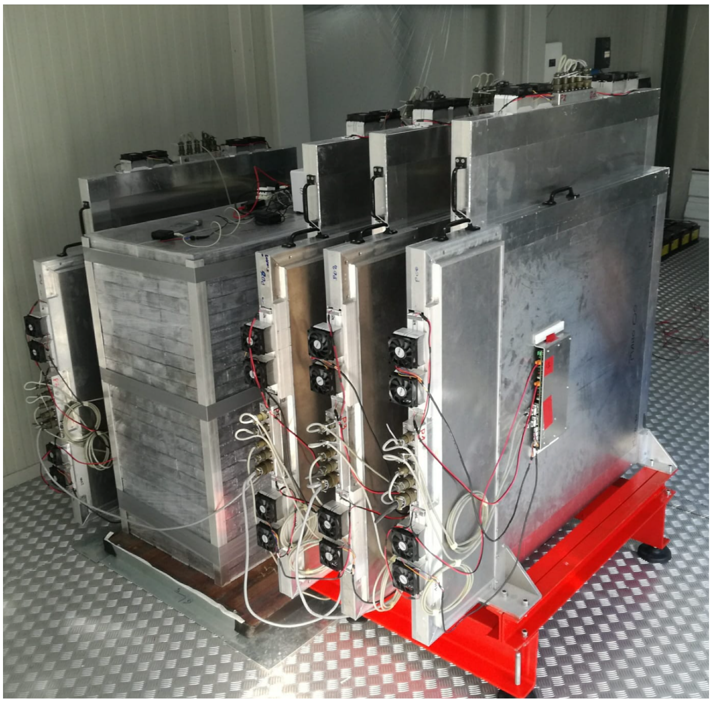

Figure 1. One of the three hodoscopes of the MURAVES experiment.

2 The MURAVES detector

The MURAVES complete detection apparatus consists in an array of three identical and completely independent tracking hodoscopes (based on the MU-RAY prototype [12–14]) each of which has an area of 1 m^2 (fig.1). The choice of installing three muon trackers is motivated by the aim of decreasing the total required exposure time, that will be anyway of one or two years. In the next paragraphs a description of the system is given with some details.

2.1 The muon hodoscope

Each MURAVES hodoscope consists of four pairs of tracking planes measuring the X and the Y coordinate by means of orthogonal plastic scintillator bars. Each plane has a sensitive area of 1 m^2. The bars have been produced at the NICADD laboratory in Fermilab [15]. Wavelength shifting (WLS) optical fibers run inside each bar along its axis, to convey the light towards the photosensors. The bars (fig. 2) have a triangular shape, with a base of 33 mm and height 17 mm, that allows an improvement of the spatial resolution (3 mm) with respect to the case of rectangular shape, thanks to the possibility of performing a weighted average of the signal given by two adjacent, partially superimposed bars. A single plane consists of two assembled modules, each composed of 32 scintillator bars. The scintillator plastic is made of a bulk of polystyrene with the addiction of PPO and POPOP scintillation dopants emitting in the blue wavelength region with an emission maximum at 420 nm. The adopted fibers are 1.2 mm diameter multiclad Kuraray Y11 S-35 fibers, characterized by an absorption spectrum approximately in the wavelength range 400 ÷ 470 nm and an emission spectrum in the range 470 ÷ 550 nm, with a peak in the green. Each pair of X-Y planes

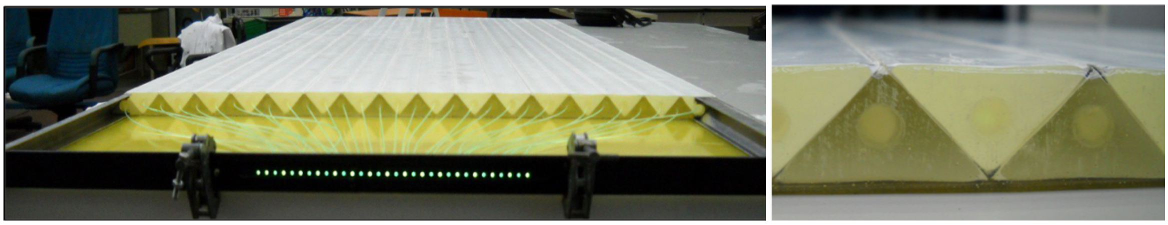

Figure 2. A MURAVES module of 32 scintillation bars with the WLS fibers inside. A detail of the bars without fibers (right).

are coupled in a self-supporting structure, giving the complete information on the point intercepted by the particle.

2.2 The photosensors and the readout system

The light propagating along the WLS fibers is read out by photosensors, one coupled to each fiber. The photosensors have been chosen to be sensitive to the WLS emission spectrum. The photosensors are ASD-RGB1C-P Silicon PhotoMultipliers (SiPM), produced by the Advansid company. Some relevant parameters of these SiPM model are reported in table 1. The photosensors are organized in arrays of 32 elements placed on a hybrid printed circuit (one for each detector module), shown in fig. 3.

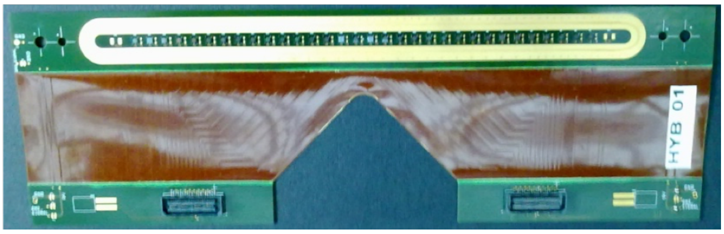

Figure 3. Hybrid board with 32 SiPMs haused.

Table 1. Relevant parameters of the Advansid SiPM ASD-RGB1C-P.

Dark Counts (DCR) (kHz/mm^2)	< 100
Photon Detection Efficiency (PDE) (%)	32.5
Operating Voltage (V)	30
Gain	2.6 $\times 10^6$
Breakdown Voltage Temperature Coefficient (mV/°C)	27

The readout system is based on a Master-Slave architecture, consisting of one Slave board for each detector module and a single Master board capable of handling up to 32 Slaves. The Master board provides data formatting and storage, data transmission and the particle trigger for the readout. Each hybrid circuit sends electric pulses (converted photon signals) to a Slave board that is equipped by a dedicated ASIC, the OMEGA EASIROC chip (Extended Analogue SI-pm ReadOut Chip [16]) which is a front-end device dedicated to the readout of SiPMs. It has 32 channels, so it can serve the 32 SiPMs corresponding to a module of the hodoscope. Each Slave provides voltage biasing of the SiPMs, amplification, discrimination and ADC conversion of the signals. The Master board is realized using a custom-programmed FPGA coupled to a stand-alone Raspberry Pi computer. The power consumption of the whole readout system is about 3 W for a Slave and 5 W for the Master. In these conditions the maximum sustainable trigger rate is ~ 270 Hz.

2.3 The thermal stabilization system

The environmental conditions present on the mountain side can be very inhospitable and strongly varying during the same day and from season to season. In addition, the very low rate of muons going through the volcano implies the need of a very long data taking period, so that the detector and all related technologies have to be stable and independent from environmental parameter variations (humidity, temperature...). Due to these requirements, a temperature control system has been designed to keep the SiPM operating temperature stable and adjustable. The SIPMs are indeed quite sensitive to temperature variations. The dependence on the temperature of the breakdown voltage is quantified by the Breakdown Voltage Temperature Coefficient (BDTC) that for the selected SiPM is BDTC = 27 mV/ °C (see table 1). The temperature control system (fig. 4) is a thermoelectric system based on the Peltier effect, capable of both cooling and heating the photosensors. Each hybrid circuit is connected with two Peltier cells and a copper bar ensures an optimal heat exchange between these Peltier elements and the SiPMs. A custom circuit controls the thermoelectric cells by the use of Pulse Width Modulation drivers to pilot the Thermal Electric Coolers with maximum efficiency. The board is connected to the outside world through an USB and a CAN Bus. With this system, temperature differences with respect to the environment of about 20 °C are achievable, with 0.1 °C stability. This system needs only a maximum of 15-20 W (including the heat exchanger ventilation) per layer, but, in order to reduce this consumption, the maximum allowed temperature difference with respect to the environment is 5 °C. Different working temperatures have been envisaged for the SiPM (working points) and an algorithm automatically changes the working point based on this requirement. In this way the maximum consumption is reduced to about 5 W per layer.

3 The Vesuvius laboratory

The installation site has been chosen according to the best achievable imaging performances and to some logistic features, such as the ease of access and the room for the installation of the entire system. According to these criteria, the site known as *Casina di Amelia* has been chosen. From this location it is possible to include in the image the bottom of the crater. A series of feasibility studies has been performed, aiming to a good compromise between signal and noise level for the chosen site.

The installation concerned the container shown in fig. 5, having an area of 45 square meters. Four locations are arranged for the hodoscopes, three pointing to the crater and one dedicated to the free-sky calibration of the hodoscopes. Each hodoscope has a 60 cm thick lead wall between the two downstream pairs of tracking planes, in order to discriminate the background due to particles

Figure 4. Temperature control system, before and after mounting on the detectors.

different from muons or to low energy muons scattered through the rock. The lead has a weight of 35 tons in total. The lead has been provided by the decommissioning of the OPERA experiment [17] at the Gran Sasso Laboratory.

The planes of the hodoscopes have been arranged at different heights to better point to the Vesuvius crater in the angular range of interest for the measurement.

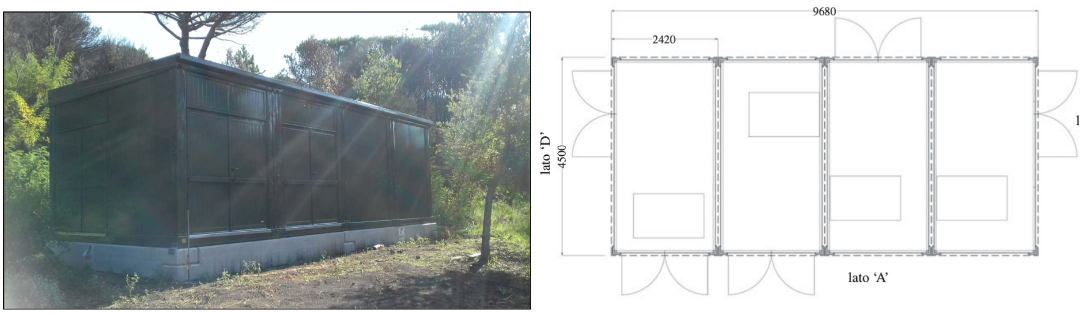

Figure 5. The container installed on the flank of the Mt. Vesuvius and the planit of its interior.

As there is no electrical power available on the site, a solar panel system has been installed on the container roof, with back-up batteries to ensure power supply during nights.

The operation of the power supply system is monitored online; it is possibile to check the status of the batteries, the power offered by solar energy, and the power consumption of the system.

At present, two of the three hodoscopes have already been installed inside the container. The first one, call it *Rosso*, has been taken on the Vesuvius in February 2019 and directed to the sky for calibration until July 2019 when it has been oriented toward the Volcano's crater. The second one, call it *Nero*, has been installed in the late July 2019, pointing to the volcano. We will need later to move also *Nero* in calibration mode. Both detectors are fully operating and aquiring data, while the third detector, named *Blu*, is under test in the laboratory at the Physics department of the University of Naples Federico II, and it is almost ready to be installed inside the container.

Figure 6. Power supply system. Left: solar panels on the roof of the container. Right: batteries inside the cointainer.

4 Data analysis strategy and expectations

When they pass through matter muons loose energy. The probability of emerging from a specific thickness of material depends on both the opacity $X = x\rho$, where ρ is the average density of the crossed material and x is the muon path through the material, and on the initial energy of the particles. The minimal energy needed to cross a certain amount of material can be estimated by knowing the physical processes that regulate the energy loss and the opacity.
Muon radiography provides a single bi-dimentional projective measurement from the detetor location, by measuring the muon flux exiting the target object along the various directions. To obtain the measurement of interest, i.e. the mass distribution inside the body, one has to get ρ from the measured quantity:

$$N(\theta, \phi) = \Delta T \times S_{eff}(\theta, \phi) \times I(\theta, X(\rho)) \tag{4.1}$$

where

$$I(\theta, X(\rho)) = \int_{E_{min}(X(\rho))}^{\infty} \Phi(\theta, E) dE \tag{4.2}$$

is the integrated muon flux. $N(\theta, \phi)$ is the measured number of muons in the direction (θ, ϕ), where θ is the angle with respect to the vertical, and depends on the integrated flux, the acquisition time and effective surface $S_{eff}(\theta, \phi) = S\epsilon A(\theta, \phi)$, i.e. the product between the sensitive area S, the geometrical acceptance $A(\theta, \phi)$ and the global efficiency ϵ. Since the minimal energy a muon needs to exit the thickness x of rock depends on the opacity, X can be evaluated from the measured $N(\theta, \phi)$, and the average density ρ can be obtained from it.
Dedicated measurement campaigns of *free-sky* muons, which means the muon flux when no object is interposed between the detector and the sky, are also performed, by pointing (in this case) the telescope to the opposite direction with respect to the cone of the volcano.
The thickness distribution along the mountain profile is evaluated from Digital Elevation Model (DEM) of the investigated data [18]. Fig. 7 shows the projection of the thickness distribution of the Vesuvius as seen from the telescope location (considered as *point-like*).
After collecting events, according to the trigger logic which requests the time coincidence of signals

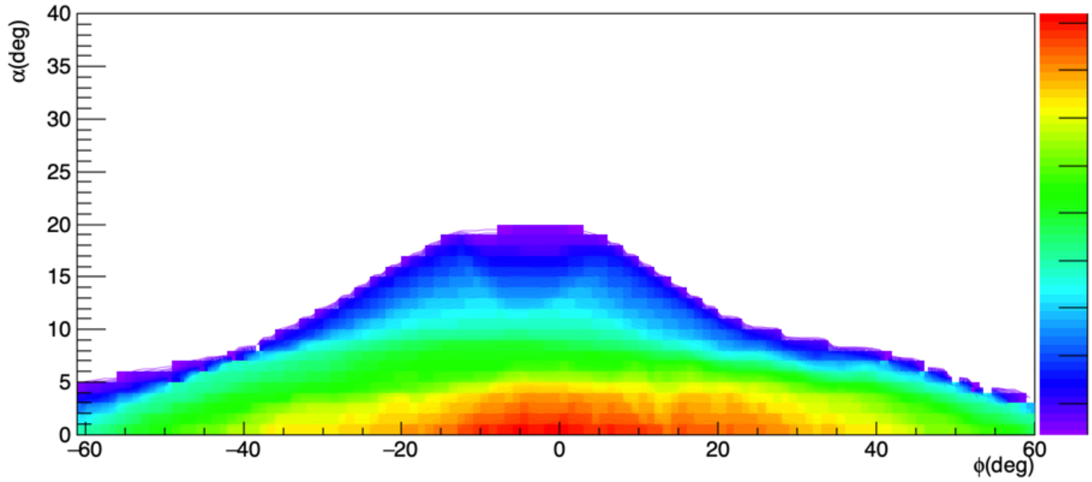

Figure 7. Vesuvius thickness map from the detector position (m).

in each of the eight planes of an hodoscope, an offline analysis is performed. It consists of the following steps:

- signal clustering;
- tracking;
- quality selection.

The clustering algorithm consists in the selection of the fired strips if they exceed a suitable energy threshold, and in the building of clusters if two or more adjacent scintillator bars are hit. These clusters are used to perform a combinatorial track fit over all the possible combinations of clusters, one for each plane and separately in the *zx* and *xy* planes. At the end of the analysis a selection is applied to exclude noise contamination and low-quality events.
Another aspect of the MURAVES analysis is the simulation of the expected flux; based on the Gaisser's modified formula [19] [20] for the *free-sky* muon flux at sea level. The simulated flux distribution accross the body of the volcano has been obtained using the PUMAS tool [21], which provides the expected absorbtion, given the thickness and the average density of the rock. This tool has the advantage of taking into account the scattering of muons through the mountain that is one of the hardest background sources to identify. To obtain the expected flux we fixed a constant density value, corresponding to the density of standard rock, 2.65 g·cm^{-3}. Fig. 8 shows the expected flux reaching the telescope, including the effect of the geometrical acceptance. The simulation of cosmic muon flux is useful for both knowing what we expect to see and to obtain a relative measure of the density distribution with respect to a specific value taken as reference. Once the data taken will be enough to keep the statistic uncertainty low, a measurement of the relative transmission, $R = \frac{N_\mu^{obs}}{N_\mu^{exp}}$ can be performed to point out any possible deviation of the observed density of the volcano from the standard rock density.

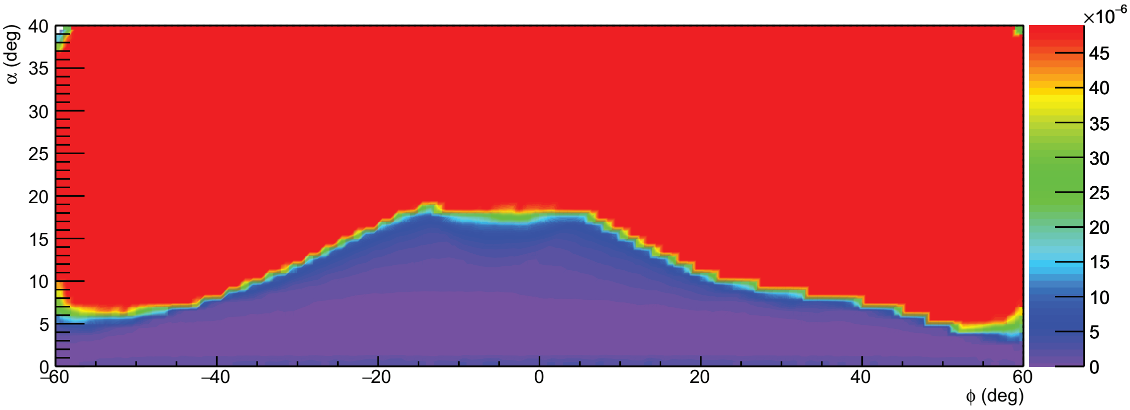

Figure 8. Expected muon flux through Vesuvius (s^{-1} m^{-2} deg^{-2}).

5 Conclusion

The MURAVES project has been designed to attempt a muon radiography of the uppermost part of the Vesuvius crater. The apparatus consists in a telescope of a total sensitive area of 3 m^2, divided in three indipendent hodoscopes of 1 m^2. The detector sensitive elements are scintillator bars coupled with WLS fibers and read by SiPM arrays. The installation of the system on the chosen site on the flank of the Volcano is already started. The data acquisition is extimated to last one or two years to achieve the needed sensitivity on density variations in the summital cone of Mt. Vesuvius. At present, two of the three hodoscopes are already fully operating inside the container, both pointing to the volcano. The first, *Rosso*, has been installed in February 2019, and, after a calibration phase of *free-sky* acquisition it has been moved toward the volcano side in July 2019 when the second hodoscope, *Nero* has been installed; the third, *Blu* is also near to be installed.
The results of this experiment could be a new confirmation of the validity of muography in the field of volcanology. They can be combined with standard gravimetric data providing a significant improvement on the spatial sensitivity in the evaluation of the density distribution.

Acknowledgments

We would like to acknowledge the INFN laboratory of Gran Sasso and the OPERA experiment Spokeperson Prof. Giovanni De Lellis for having provided in kind the lead inserted in the detectors. We also thank the Laboratory of Geomatics of INGV, Osservatorio Vesuviano for processing the DTM data.
Special thanks go to all the technical personnel that supported the design and the implementation of the experiment.

References

[1] L. W. Alvarez *et al.*, *Science* 167 (1970) 832

[2] H. K. M. Tanaka, T. Kusagaya, H. Shinohara, *Nature Communications* 5 (2014) 3381

[3] H. K. M. Tanaka *et al.*, *Nucl. Instrum. Methods A* 575 (2007) 489-497

[4] H. K. M. Tanaka *et al.*, *Earth and Planetary Science Letters* 263 (2007) 104-113

[5] H. K. M. Tanaka, M. Ohshiro, *Geosci. Instrum. Method. Data Syst.* 5 (2016) 427-435

[6] F. Ambrosino *et al.*, *J. of Geophys. Res.: Solid Earth* 120 (2015) 7290-7307

[7] N. Lesparre *et al.*, *Geophys. J. Int.* 190 (2012) 1008-1019

[8] C. Carloganu *et al.*, *Geosci. Instrum. Method. Data Syst.* 2 (2013) 55-60

[9] F. Ambrosino *et al.*, *JINST* 9 (2014) C02029

[10] L. Cimmino *et al.*, *Annals of Geophysics* 60 (2017) S0104

[11] G. Saracino *et al.*, *Annals of Geophysics* 60 (2017) S0102

[12] G. Ambrosi *et al.*, *Nucl. Instrum. Methods A* 628 (2011) 120-123

[13] A. Anastasio *et al.*, *Nucl. Instrum. Methods A* 732 (2013) 423-426

[14] A. Anastasio *et al.*, *Nucl. Instrum. Methods A* 718 (2013) 134-137

[15] A. Pla-Dalmau, A.D. Bross and K.L. Mellot, Extruded Plastic Scintillation Detectors, FERMILAB-Conf-99/095

[16] S. Callier *et al.*, *Phys. Procedia* 37 (2012) 1569-1576

[17] R Acquafredda *et al.*, *JINST* 4 (2009) P04018

[18] Digital Terrain Model (DTM) of the Campania Region at 1:5000 scale. Laboratory of Geomatics INGV-OV. Educational Licence by Campanian Region number 2, 16/06/2006. http://sit.regione.campania.it/portal/portal/default/Cartografia

[19] T. Gaisser, *Cambridge University Press, New York* (1990)

[20] A. Tang *et al.*, *Phys. Rev.* D 74, 053007 (2016)

[21] V. Niess *et al.*, *Computer Physics Communications* 229 (2017) 54-67